Available online at www.sciencedirect.com
ScienceDirect
Journal of the European Ceramic Society 29 (2009) 85–90
www.elsevier.com/locate/jeurceramsoc

Ni–YSZ cermet micro-tubes with textured surface

R. Campana, A. Larrea*, J.I. Peña, V.M. Orera

Instituto de Ciencia de Materiales de Aragón, ICMA, CSIC-Universidad de Zaragoza, Zaragoza 50009, Spain

Received 28 March 2008; received in revised form 30 May 2008; accepted 11 June 2008
Available online 22 July 2008

Abstract

Tubular Ni–YSZ porous cermets, with the external surface textured in the form of submicron size alternating YSZ and porous Ni lamellae aligned perpendicular to the tube surface have been fabricated. The surface of the ceramic tubes of eutectic composition was directionally solidified in the radial direction using the laser zone melting procedure where the power of the laser was adjusted to melt a thin surface layer. The melt solidified in the very high thermal growth radial gradient produced by radiation losses and convention cooling. A crack free layer with typical eutectic lamellar microstructure, with domains aligned perpendicular to the tube surface, was produced along the external surface of the tubes. The porous cermet tubes were prepared by thermo-chemical reduction of the NiO phase in the previously textured binary NiO–YSZ eutectic precursors. After reduction, porous Ni leaves of about 100 nm lateral dimension were confined between the YSZ lamellae in the textured layer. The influence of growth parameters over microstructure size and morphology is discussed.
© 2008 Elsevier Ltd. All rights reserved.

Keywords: Microstructure-final; ZrO_2; Fuel cells; Laser zone melting

1. Introduction

Porous cermets find application in electrochemistry, including catalysers and fuel cells, and for this reason there has been a growing interest in the past few years in these materials. In particular, Ni–YSZ cermets find application as catalysers for steam reforming of methane (SRM), methane reforming catalyst (MRC), partial oxidation of methane (POM), in this case with the addition of Ce, and as solid oxide fuel cells (SOFC) anodes. Very often tubular geometry is chosen because of the better thermo-mechanical behaviour and sealing simplicity compared to other geometries. Reduction of tube diameter also increases the reaction area density and gas permeation through the tube wall and reduces heating-up times.[1–3]

Electrochemical performance of cermets is a function of the number of triple phase boundaries (TPBs) where reactant gases and electrons meet. They have to be porous in order to allow transport of reactant and product species with a good connectivity between pores and metal. The morphology and size of the pores and metallic particles as well as the microstructure stability under operation, are some critical factors for the applicability of these porous cermets.[4] Additionally, in electro-ceramic devices only a small volume region near to the reactant gases interface takes place in electrochemical reactions, the so-called functional layer of about 20-μm thickness.

Recently, the production of channelled Ni– and Co–YSZ porous cermets by reduction of NiO– and CoO–YSZ directionally solidified eutectics has been reported.[5–7] Directionally solidified eutectics are characterized by the presence of a self-assembled homogeneous and periodic microstructure, with clean and strong interfaces.[8] In this case, by alternating NiO (CoO) and YSZ lamellae whose size can be controlled by the processing parameters. Reduction of the eutectic microstructure leads to channelled Ni(Co)–YSZ porous cermets with alternating porous metal and YSZ lamellae that provide good electrical conductivity, gas permeation and a suitable thermal expansion coefficient for convenient thermo-mechanical integration in the SOFC. As mentioned above it is very important for electrochemical applications that the electrode microstructure remains stable at the working temperature. During cell operation Ni particles tend to agglomerate due to the poor wettability between metallic Ni and the ceramic phase. Ni coarsening decreases the electrical conductivity and the electrocatalytic activity of the anode. However, we have shown that the cermets prepared from directionally solidified eutectics offer high resistance to metal coarsening under operation. In previous works we verified that the electrical

* Corresponding author.
E-mail address: alarrea@unizar.es (A. Larrea).

0955-2219/$ – see front matter © 2008 Elsevier Ltd. All rights reserved.
doi:10.1016/j.jeurceramsoc.2008.06.005

conductivity and the pore size distribution present no degradation after 300 h at 900 °C under a H_2/N_2 atmosphere.[9,6] This is a consequence of the channelled microstructure of the cermet and of the low-energy metal–ceramic interfaces resulting from reduction of directionally solidified eutectics.[10]

The general purpose of this work is to demonstrate the usefulness of eutectic growth for the preparation of ceramic tubes with appropriate textured external layer. In particular our aim was to develop fabrication technology of electro-ceramic materials for producing a thin layer of channelled Ni–YSZ porous cermet on the surface of conventional ceramic Ni–YSZ micro-tubes, with the complementary objective of getting narrow channels oriented along the radial direction. Specifically, a functional layer totally integrated on the tubular substrate and with a geometrical phase disposition to fulfil two main requirements, high specific area and good gas and charged species flow perpendicular to the outer surface of the device. For this purpose we used a procedure similar to the one we developed for texturing planar surfaces but modified for cylindrical surfaces.[11,12]

The Ni–YSZ cermets were produced following a three-step procedure. The first step was the fabrication of NiO–YSZ microtubes with the eutectic composition. The external surface of the tubes was melted to the required depth using a CO_2 laser heating source in a second step. Crystal growth kinetics of the binary eutectic was studied to determine the eutectic microstructure and the cracking behaviour as a function of processing parameters. Once the desired microstructure was obtained NiO was reduced to metallic Ni, a process which is very fast and efficient in YSZ composites.

2. Experimental procedures

Ceramic cylinders of NiO–YSZ eutectic composition about 120 mm in length, 3 mm in diameter, and 400 μm wall thickness, were prepared following the procedure schematised in Fig. 1. As starting materials we used NiO (99.99% Sigma–Aldrich, St. Louis, MO) and 8YSZ (8 mol% Y_2O_3-stabilised ZrO_2, 99.9% purity, Tosoh, Tokyo, Japan). The NiO powders were milled twice to decrease their grain size and then mechanically mixed with 8YSZ. The density of green ceramics was about 40%. Two sets of samples, dense and porous, were prepared as follows: fully dense ceramics were sintered at 1500 °C dwell time 2 h; porous ceramics were prepared with addition of 1.5 wt% starch to the slurry and sintered at 1350 °C dwell time 2 h. The density of the latter was 70% and the size of pores about 5 μm as measured by Hg-porosimetry. The composition of the full dense ceramics is about 56.5 vol% NiO and 43.5 vol% YSZ. Reduction of NiO was performed at 750 °C for 3 h in H_2/Ar mixture (5 vol%). It produces cermets with 43.5 vol% YSZ, 33.1 vol% of metallic Ni and 23.4 vol% of pores. This pore volume can be increased up to about 50 vol% for the cermets obtained from porous precursors.

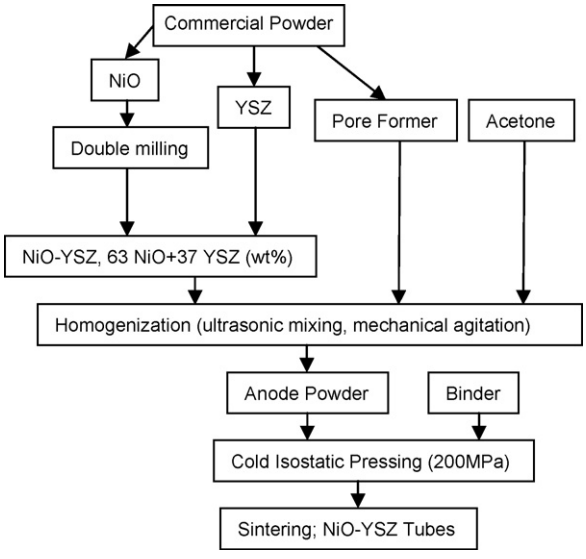

Fig. 1. Fabrication steps of NiO–YSZ tubes with the eutectic composition.

Directional solidification of the tube surfaces was performed in a laser float zone apparatus using a 600 W CO_2 Blade laser (10.6 μm wavelength) at different growth rates between 10 and 1000 mm/h. The laser beam is transformed by a reflexi-cone optical device into a focussed ring about 1 mm in length on the tube surface. The tubes are rotated at different rates between 10 and 300 rpm (revolutions/min) inside the growth chamber. A pre-heating of about 600 °C was provided by a focussed conventional halogen 300 W lamp in order to decrease the thermal shock. Details of the laser processing apparatus can be found elsewhere.[13]

The microstructure of the samples was studied by optical microscopy (OM) and scanning electron microscopy (SEM). SEM images of polished samples previously infiltrated with a low density resin were obtained in a JEOL 6400 microscope. The microstructure is homogeneous with typical cellular-lamellar microstructure. The phase interspacing was obtained from the backscatter electron SEM images. DC electrical conductivity of the processed tubes was performed using the four-point arrangement with Pt paste electrodes in the processed surface and a 220 Keithley current source and an HP 34401A microvoltmeter.

3. Laser processing

The main and most difficult objective of this research was to obtain a homogeneous non-cracked coating of NiO–YSZ with fine, aligned structures on the external surface of the tubes. We were also looking for some control to be exerted over the morphology, orientation and size of the phases. In the case of directional solidification, this control can be achieved, to a certain extent, by choosing the appropriate conditions for solidification of the eutectic melt. In fact, the microstructure of directionally solidified eutectics (DSE) is a consequence of the balance between cooperative eutectic growth and the growth habits of each particular phase (Ref. [8], and references herein). If cooperative growth dominates, the microstructure expected for this composition should be regular, with alternating NiO and YSZ lamellae aligned along the direction of the solidification gradient. For small values of the eutectic Peclet number $Pe = v\lambda/2D \ll 1$ (D is the diffusion constant in the melt), the following relationship holds between inter-phase spacing λ and

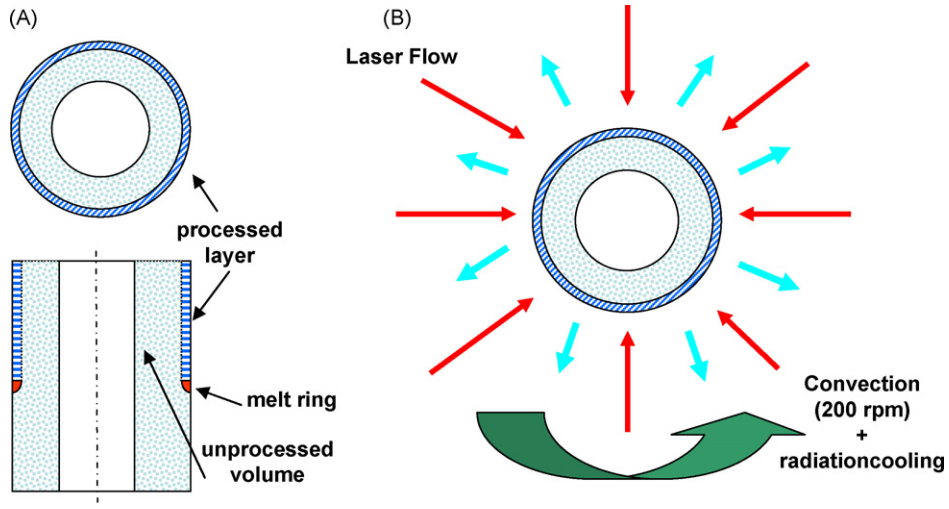

Fig. 2. Scheme of the processing set-up. (A) Transverse and longitudinal cross-sections showing the precursor ceramic tube and the laser processed layer. The melt ring is displaced longitudinally along the tube surface. (B) Input energy provided by the laser beam and surface energy losses.

solidification rate v[14]

$$\lambda^2 v = K_1 \quad (1)$$

where $K_1 = 35.8\ \mu m^3/s$ for this compound.[15] And

$$\lambda\, \Delta T = K_2 \quad (2)$$

ΔT being the thermal under-cooling. According to Eq. (1) increase of the growth rate produces a refining of the eutectic microstructure and it has been used to obtain a lamellar interspacing between 3 and 0.2 μm.[16] However, thermal undercooling has to be kept at the smallest values for coupled eutectic growth, which implies high values of the growth thermal gradients G_T to growth rate ratio $G_T/v \gg 1$.[17] At higher growth rates, the microstructure changes to cellular eutectic with cells growing with their long axis aligned along the growth thermal gradient. As a conclusion, planar eutectic growth is achieved for low growth rates, small departures from the eutectic composition and large solidification thermal gradients.

Conversely, high thermal gradients are deleterious for sample processing as cracks can develop because of the high cooling rates. For rods grown by LFZ the relationship between solidification thermal gradient and sample radius R was found

$$G_T = \frac{K_3}{R^{3/2}} \quad (3)$$

K_3 being a constant. In fact, resistance to thermal shock is largely improved if the melt dimensions are reduced.[18] In our case we adjusted the growth parameters in order to melt only a thin surface layer trying to accomplish better thermal stress resistance without deteriorating the functionality of the textured functional area (see Fig. 2).

In surface melting process using a laser source two length scales are of importance, the optical length $l_\alpha = \alpha^{-1}$, α being the absorption coefficient and the thermal diffusion length l_T defined as[19]

$$l_T \approx 2\sqrt{D\tau_l} \quad (4)$$

where D is the thermal diffusivity and τ_l the laser dwell time which, for a moving DC laser source, can be approximated by ω_0/v, ω_0 being the laser spot width along the travelling direction.

The absorption coefficient of the NiO–YSZ composite at the CO_2 laser wavelength ($\approx 1000\ cm^{-1}$) is unknown but it was expected to be very large due to multi-phonon absorption ($l_\alpha < 1\ \mu m$). For fully dense ceramics, using the thermo-physical properties of YSZ–NiO in Table 1 we obtained thermal diffusion lengths of 32, 10 and 3.2 mm for growth rates of 10, 100 and 1000 mm/h respectively. As a consequence $l_\alpha \ll l_T$ and laser light is absorbed on the surface. Since laser heating dwell times are not short enough to shorten thermal diffusion length, in order to melt only a thin layer we need to reach the situation in which laser heating is nearly balanced with surface losses. This problem was studied by Shieh and Wu in YSZ[20] and they find that for deep melts, radiation heat losses resulted in surface solidification and two solidification fronts are observed, converging at about 20–30 μm from the surface. That problem disappeared for shallow melt depths which were the processing conditions we chose here.

Table 1
Thermo-physical properties of YSZ–NiO eutectics used in this work

Density (%)	Mass density, ρ (g/cm^3)	Thermal conductivity, κ (W/cm K) (1000 K)	Thermal diffusivity, D (cm^2/s) (1000 K)
100	6.35	0.033	7.2×10^{-3}
70	4.33	0.023	7.2×10^{-3}

Maxwell relationship[23] and data for ZrO_2 and NiO from Refs. [19,24] were used for calculating the thermal conductivity of composite and porous samples.

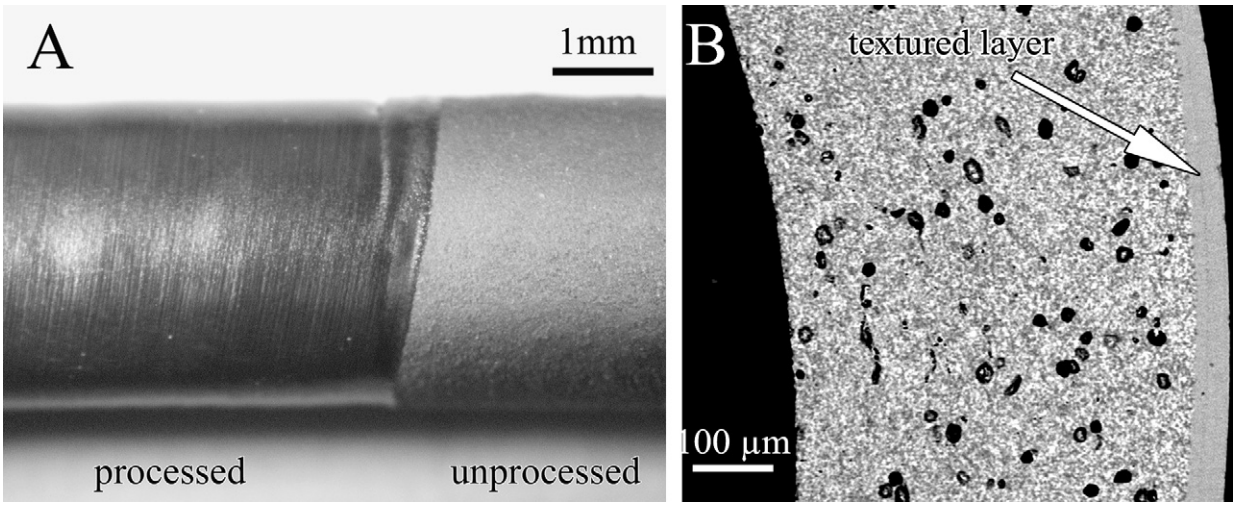

Fig. 3. (A) Optical photograph of a processed tube. (B) SEM images of transverse cross-section of a Ni–YSZ cermet processed at 400 mm/h.

4. Results and discussion

First, experiments were conducted to determine the processing conditions for which cracks were not observed in the solidified layer. Laser power was about 60 and 50 W for dense and porous substrates respectively, which corresponds to laser fluences on the sample surface of ≈320 and 260 W/cm^2. We estimated 50% optical power losses in the focusing optical setup. These laser fluences are about the threshold heating power to obtain stable melts. In fact, melting threshold is defined by the equilibrium at the substrate surface between heating and loss fluences. Main thermal loss sources are thermal radiation energy flux J_r given by the Stefan–Boltzmann equation, convection flux, J_c, and thermal conduction flux

$$J_{th} = J_{loss} = J_r + J_c + \kappa \nabla T = \varepsilon\sigma_r(T_m^4 - T_\alpha^4) + \eta(T_m - T_\alpha) + \kappa G_T^r \quad (5)$$

where $\sigma_r = 5.7 \times 10^{-12}$ W/cm^2 K^4, and for this material we took $\varepsilon = 0.85$[21] and $\eta = 75 \times 10^{-4}$ W/cm^2 K.[22]

The solution of the heat transport equation for a travelling cylinder is at least a two-dimension problem and has to be done numerically,[19] which was outside the scope of this work. However, assuming some very crude approximations to the boundary Eq. (5) we can make a rough estimation of the energy flows involved in the process. In fact, neglecting melt overheating and assuming that the radiating hot surface can be approximated by a cylinder section of 1-mm long at the eutectic melt temperature of 2123 K, $J_r \approx 100$ W/cm^2, convective losses are estimated for a cylinder of this size in air to be ≈15 W/cm^2. Conductive losses $\kappa \nabla T$ are then (Eq. (5)) 205 and 145 W/cm^2 for dense and porous substrates respectively, and according to κ-values in Table 1 the estimated thermal gradient is about 6250 K/cm, a typical value for LFZ experiments.[18] In spite of the very rough approximation to the problem we have used, we can see that the relative magnitudes involved in the tube laser processing are coherent with the expected values.

For dense substrates crack-free solidified layers were only obtained under very critical processing conditions. The 600 °C pre-heating does not seem to be enough to avoid deleterious thermal shock. For porous substrates the processed layer remains un-cracked for solidification rates above 400 mm/h and fast rotations. In Fig. 3 we show the optical photograph of a processed tube and the SEM image of its transverse cross-section. The depth of the solidified volume is between 25 and 30 μm irrespective of the pulling rate. The microstructure in the textured layer has been refined relative to that of the ceramic. It consists of alternating NiO and YSZ lamellae oriented in a direction perpendicular to the external surface. The interspacing is also quite independent of the pulling rate, between 400 and 1200 mm/h, and decreases from about 325 nm in the deepest melted volume near to the ceramic to less than 200 nm in the external surface. Interspacing values inside the solidified layer are coherent with the predictions of Eq. (1) of 400–300 nm for the pulling rates used, being in the external surface smaller than expected.

The absence of a dependence of interspacing on the pulling rate is clearly a consequence of the radial thermal gradient. In fact solidification takes place along the radial direction, starting presumably in the surface, as indicated by the high quotient between surface heat losses and thermal conduction along the tube. Displacement of the cylinder in the axial thermal gradient seems to have little effect on the microstructure which is dominated by radial solidification. In addition, the microstructure can be changed by cylinder rotation. We performed solidifications at 400 mm/h axial pulling rates and cylinder rotations of 10, 50 and 200 rpm. The depth of the processed region increased when the rotation rate decreased and the probability of layer cracking consequently increased. The average microstructural interspacing near to the surface also changes at low rotation rates being 375, 340 and 290 nm for 10, 50 and 200 rpm respectively. Notice that at low rotation rates we approach the predictions of Eq. (1). Consequently, it is evident that sample rotation plays a critical role in increasing the surface heat losses, hence in establishing a strong radial growth gradient. This is an aspect that has still to be understood from the point of view of theoretical calculations

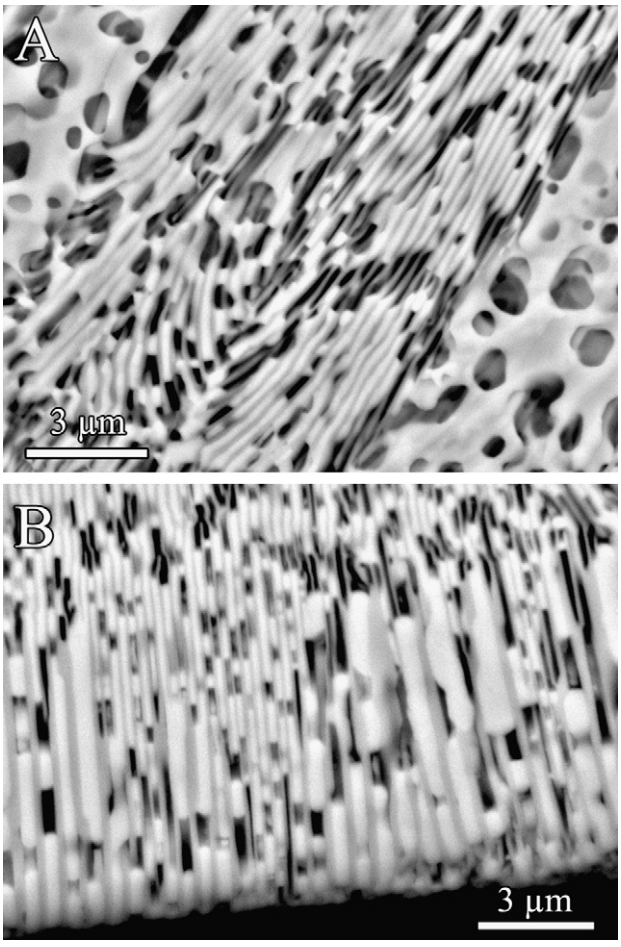

Fig. 4. SEM images of the textured layer obtained in previously infiltrated polished samples. In (A) some Ni leaves are parallel to the image plane showing their pores. In (B) the lamellae are perpendicular to the tube surface and image plane.

since current models of rotation enhanced convection predict an enhancement which scales with $(v_r)^{1/2}$, v_r being the surface tangential speed in m/s units.[19] In our case the radius of cylinder is so small that even at the highest rotation rates the effect is expected to be negligible according to that model.

After the thermo reduction treatment the NiO grains transform into metallic Ni and pores all through the sample and the NiO lamellae of the textured layer into porous Ni plates about 200–120 nm in thickness. In Fig. 4 we show two SEM images of the transverse section of a textured sample after the reduction process. In Fig. 4a some porous Ni leaves parallel to the image plane can be observed, whereas in Fig. 4b the alignment of the alternating YSZ and Ni layers perpendicular to the tube surface is apparent. The electrical resistance of processed tubes is about $7.5 \times 10^{-5}\ \Omega$ cm indicating that the Ni leaves are connected.

5. Conclusions

By reduction of laser-processed NiO–YSZ eutectic tubes it is possible to prepare porous Ni–YSZ cermets with a textured external layer. This layer is formed by nanometric size (100–200 nm) alternating YSZ and porous Ni lamellae aligned perpendicular to the tube surface. The theoretical and experimental analysis of the laser processing conditions shows that to get a crack-free textured layer with fine microstructure it is imperative to melt only a thin surface layer (25–30 μm) using high pulling rates and high rotation speeds. The good electrical conductivity, porosity and the fine microstructure aligned along the radial direction of the textured layer lead one to expect a good catalytic response of these tubes.

Acknowledgements

The results were obtained under projects financed by the Spanish Government and Feder program of the European Community: MAT2006-13005-C03-01 and CIT-120000-2007-50. We thank Dr. J. Stankiewicz for electrical measurements and Dr. R.I. Merino for useful discussions on the laser processing models.

References

1. Locket, M., Simmons, M. J. H. and Kendall, K., CFD to predict temperature profile for scale up of micro-tubular SOFC stacks. *J. Power Sources*, 2004, **131**, 243–246.
2. Kendall, K. and Palin, M., A small solid oxide fuel cell demonstrator for microelectronic applications. *J. Power Sources*, 1998, **71**, 268–270.
3. Sammes, N. M., Du, Y. and Bove, R., Design and fabrication of a 100 W anode supported micro-tubular SOFC stack. *J. Power Sources*, 2005, **145**, 428–434.
4. Lee, J. H., Heo, J. W., Lee, D. S., Kim, J., Kim, G. H., Lee, H. W. *et al.*, The impact of anode microstructure on the power generating characteristics of SOFC. *Solid State Ionics*, 2003, **158**, 225–232.
5. Laguna-Bercero, M. A., Larrea, A., Peña, J. I., Merino, R. I. and Orera, V. M., Structured porous Ni and Co–YSZ cermets fabricated from directionally solidified eutectic composites. *J. Eur. Ceram. Soc.*, 2005, **25**, 1455–1462.
6. Laguna-Bercero, M. A., Larrea, A., Merino, R. I., Peña, J. I. and Orera, V. M., Crystallography and thermal stability of textured Co–YSZ cermets from eutectic precursors. *J. Eur. Ceram. Soc.*, 2008, **28**, 2325–2329.
7. Alem, N., Dravid, V. P. and Li, S., Characterization of $Ni_xCo_{1-x}O/ZrO_2(CaO)$ directionally solidified eutectic (DSE) ceramic composites with a ductile interphase. *J. Mater. Res.*, 2007, **22**, 1797–1805.
8. LLorca, J. and Orera, V. M., Directionally solidified eutectic ceramic oxides. *Prog. Mater. Sci.*, 2006, **51**, 711–809.
9. Laguna-Bercero, M. A., Larrea, A., Peña, J. I., Merino, R. I. and Orera, V. M., Stability of channeled Ni–YSZ cermets produced from self-assembled NiO–YSZ directionally solidified eutectics. *J. Am. Ceram. Soc.*, 2005, **88**, 3215–3217.
10. Laguna-Bercero, M. A. and Larrea, A., Interface-induced crystallographic reorientation of Ni particles in Ni–YSZ cermets. *J. Am. Ceram. Soc.*, 2007, **90**, 2954–2960.
11. Larrea, A., de la Fuente, G. F., Merino, R. I. and Orera, V. M., ZrO_2–Al_2O_3 eutectic plates produced by laser zone meeting. *J. Eur. Ceram. Soc.*, 2002, **22**, 191–198.
12. Merino, R. I., Peña, J. I., Laguna-Bercero, M. A., Larrea, A. and Orera, V. M., Directionally solidified calcia stabilised zirconia-nickel oxide plates in anode supported SOFC's. *J. Eur. Ceram. Soc.*, 2004, **24**, 1349–1353.
13. Peña, J. I., Merino, R. I., de la Fuente, G. F. and Orera, V. M., Aligned ZrO_2(c)–$CaZrO_3$ eutectics grown by the laser floating zone method: electrical and optical properties. *Adv. Mater.*, 1996, **8**, 909–912.
14. Hunt, J. D. and Jackson, K. A., Binary eutectic solidification. *Trans. Metal. Soc. AIME*, 1966, **236**, 843–852.
15. Merino, R. I., Peña, J. I., Larrea, A, de la Fuente, G. F. and Orera, V. M., Melt grown composite ceramics obtained by directional solidification: structural and functional applications. *Recent Research Developments in Materials*

Science, 2003, vol. 4, pp. 1–24. Research Singhpost, Kerala, India ISBN: 81-271-0022-6.
16. Laguna-Bercero, M. A., Cermets texturados de Ni–YSZ y Co–YSZ para ánodos de SOFC. PhD Dissertation, Dpto. de Física de la Materia Condensada. Universidad de Zaragoza; 2005.
17. Burden, M. H. and Hunt, J. D., Cellular and dendritic growth. *J. Cryst. Growth*, 1974, **1974**(22), 99–108.
18. Peña, J. I., Merino, R. I., Harlan, N. R., Larrea, A., de la Fuente, G. F. and Orera, V. M., Microstructure of Y_2O_3 doped Al_2O_3–ZrO_2 eutectics grown by the laser floating zone method. *J. Eur. Ceram. Soc.*, 2002, **22**, 2595–2602.
19. Bäuerle, D., *Laser Processing and Chemistry*. Springer-Verlag, Berlin, Heidelberg, New York, 2000 [chapters 2 and 10].
20. Shieh, J.-H. and Wu, S.-T., Rapid solidification of a plasma-sprayed ceramic coating melted by a CO_2-laser. *Appl. Phys. Lett.*, 1991, **59**, 1512–1514.
21. Merino, R. I., Measured at 1000 °C with a two colours pyrometer. Private communication.
22. Ester, F. and Peña, J. I., Analysis of the molten zone in the growth of the Al_2O_3–$ZrO_2(Y_2O_3)$ eutectic by the laser floating zone technique. *Bol. Soc. Esp. Ceram. Vidrio*, 2007, **46**, 240–246.
23. Kingery, W. D., Bowen, H. K. and Uhlmann, D. R., *Introduction to Ceramics*. John Wiley & Sons, New York, 1975, p. 636.
24. Watanabe, H., Thermal constants for Ni, NiO, MgO, MnO and CoO at low-temperatures. *Thermochim. Acta*, 1993, **218**, 365–372.